

# Observation of two charged bottomonium-like resonances in $\Upsilon(5S)$ decays

- A. Bondar,<sup>1</sup> A. Garmash,<sup>1</sup> R. Mizuk,<sup>16</sup> D. Santel,<sup>3</sup> K. Kinoshita,<sup>3</sup> I. Adachi,<sup>10</sup> H. Aihara,<sup>52</sup> K. Arinstein,<sup>1</sup> D. M. Asner,<sup>41</sup> T. Aushev,<sup>16</sup> T. Aziz,<sup>48</sup> A. M. Bakich,<sup>47</sup> E. Barberio,<sup>29</sup> K. Belous,<sup>14</sup> V. Bhardwaj,<sup>42</sup> M. Bischofberger,<sup>32</sup> A. Bozek,<sup>36</sup> M. Bračko,<sup>27,17</sup> T. E. Browder,<sup>9</sup> M.-C. Chang,<sup>4</sup> P. Chang,<sup>35</sup> A. Chen,<sup>33</sup> B. G. Cheon,<sup>8</sup> K. Chilikin,<sup>16</sup> R. Chistov,<sup>16</sup> I.-S. Cho,<sup>57</sup> K. Cho,<sup>20</sup> S.-K. Choi,<sup>7</sup> Y. Choi,<sup>46</sup> J. Dalseno,<sup>28,49</sup> M. Danilov,<sup>16</sup> Z. Doležal,<sup>2</sup> A. Drutskoy,<sup>16</sup> S. Eidelman,<sup>1</sup> D. Epifanov,<sup>1</sup> J. E. Fast,<sup>41</sup> V. Gaur,<sup>48</sup> N. Gabyshev,<sup>1</sup> Y. M. Goh,<sup>8</sup> B. Golob,<sup>25,17</sup> T. Hara,<sup>10</sup> K. Hayasaka,<sup>31</sup> Y. Hoshi,<sup>50</sup> H. J. Hyun,<sup>23</sup> T. Iijima,<sup>31,30</sup> K. Inami,<sup>30</sup> A. Ishikawa,<sup>51</sup> M. Iwabuchi,<sup>57</sup> Y. Iwasaki,<sup>10</sup> T. Iwashita,<sup>32</sup> T. Julius,<sup>29</sup> J. H. Kang,<sup>57</sup> T. Kawasaki,<sup>38</sup> H. Kichimi,<sup>10</sup> C. Kiesling,<sup>28</sup> J. B. Kim,<sup>21</sup> J. H. Kim,<sup>20</sup> K. T. Kim,<sup>21</sup> M. J. Kim,<sup>23</sup> Y. J. Kim,<sup>20</sup> B. R. Ko,<sup>21</sup> N. Kobayashi,<sup>53</sup> S. Koblitz,<sup>28</sup> P. Kodyš,<sup>2</sup> S. Korpar,<sup>27,17</sup> P. Križan,<sup>25,17</sup> T. Kuhr,<sup>19</sup> R. Kumar,<sup>42</sup> T. Kumita,<sup>54</sup> A. Kuzmin,<sup>1</sup> J. S. Lange,<sup>5</sup> S.-H. Lee,<sup>21</sup> J. Li,<sup>45</sup> Y. Li,<sup>56</sup> J. Libby,<sup>11</sup> C. Liu,<sup>44</sup> Z. Q. Liu,<sup>12</sup> D. Liventsev,<sup>16</sup> R. Louvot,<sup>24</sup> D. Matvienko,<sup>1</sup> S. McOnie,<sup>47</sup> H. Miyata,<sup>38</sup> Y. Miyazaki,<sup>30</sup> G. B. Mohanty,<sup>48</sup> A. Moll,<sup>28,49</sup> N. Muramatsu,<sup>58</sup> R. Mussa,<sup>15</sup> M. Nakao,<sup>10</sup> Z. Natkaniec,<sup>36</sup> S. Neubauer,<sup>19</sup> M. Niijyama,<sup>22</sup> S. Nishida,<sup>10</sup> K. Nishimura,<sup>9</sup> O. Nitoh,<sup>55</sup> T. Nozaki,<sup>10</sup> S. L. Olsen,<sup>45</sup> Y. Onuki,<sup>51</sup> P. Pakhlov,<sup>16</sup> G. Pakhlova,<sup>16</sup> H. Park,<sup>23</sup> H. K. Park,<sup>23</sup> T. K. Pedlar,<sup>26</sup> M. Petrič,<sup>17</sup> L. E. Piilonen,<sup>56</sup> A. Poluektov,<sup>1</sup> M. Prim,<sup>19</sup> M. Ritter,<sup>28</sup> M. Röhrken,<sup>19</sup> S. Ryu,<sup>45</sup> H. Sahoo,<sup>9</sup> Y. Sakai,<sup>10</sup> D. Santel,<sup>3</sup> T. Sanuki,<sup>51</sup> O. Schneider,<sup>24</sup> C. Schwanda,<sup>13</sup> K. Senyo,<sup>30</sup> M. E. Sevier,<sup>29</sup> M. Shapkin,<sup>14</sup> V. Shebalin,<sup>1</sup> T.-A. Shibata,<sup>53</sup> J.-G. Shiu,<sup>35</sup> B. Schwartz,<sup>1</sup> F. Simon,<sup>28,49</sup> P. Smerkol,<sup>17</sup> Y.-S. Sohn,<sup>57</sup> A. Sokolov,<sup>14</sup> E. Solovieva,<sup>16</sup> M. Starič,<sup>17</sup> M. Sumihama,<sup>6</sup> T. Sumiyoshi,<sup>54</sup> S. Tanaka,<sup>10</sup> G. Tatishvili,<sup>41</sup> Y. Teramoto,<sup>39</sup> I. Tikhomirov,<sup>16</sup> M. Uchida,<sup>53</sup> S. Uehara,<sup>10</sup> T. Uglov,<sup>16</sup> Y. Ushiroda,<sup>10</sup> S. E. Vahsen,<sup>9</sup> G. Varner,<sup>9</sup> A. Vinokurova,<sup>1</sup> C. H. Wang,<sup>34</sup> M.-Z. Wang,<sup>35</sup> P. Wang,<sup>12</sup> X. L. Wang,<sup>12</sup> Y. Watanabe,<sup>18</sup> K. M. Williams,<sup>56</sup> E. Won,<sup>21</sup> B. D. Yabsley,<sup>47</sup> Y. Yamashita,<sup>37</sup> M. Yamauchi,<sup>10</sup> C. Z. Yuan,<sup>12</sup> Y. Yusa,<sup>38</sup> Z. P. Zhang,<sup>44</sup> V. Zhilich,<sup>1</sup> V. Zhulanov,<sup>1</sup> A. Zupanc,<sup>19</sup> and O. Zyukova<sup>1</sup>

(The Belle Collaboration)

<sup>1</sup>Budker Institute of Nuclear Physics SB RAS and Novosibirsk State University, Novosibirsk 630090

<sup>2</sup>Faculty of Mathematics and Physics, Charles University, Prague

<sup>3</sup>University of Cincinnati, Cincinnati, Ohio 45221

<sup>4</sup>Department of Physics, Fu Jen Catholic University, Taipei

<sup>5</sup>Justus-Liebig-Universität Gießen, Gießen

<sup>6</sup>Gifu University, Gifu

<sup>7</sup>Gyeongsang National University, Chinju

<sup>8</sup>Hanyang University, Seoul

<sup>9</sup>University of Hawaii, Honolulu, Hawaii 96822

<sup>10</sup>High Energy Accelerator Research Organization (KEK), Tsukuba

<sup>11</sup>Indian Institute of Technology Madras, Madras

<sup>12</sup>Institute of High Energy Physics, Chinese Academy of Sciences, Beijing

<sup>13</sup>Institute of High Energy Physics, Vienna

<sup>14</sup>Institute of High Energy Physics, Protvino

<sup>15</sup>INFN - Sezione di Torino, Torino

<sup>16</sup>Institute for Theoretical and Experimental Physics, Moscow

<sup>17</sup>J. Stefan Institute, Ljubljana

<sup>18</sup>Kanagawa University, Yokohama

<sup>19</sup>Institut für Experimentelle Kernphysik, Karlsruher Institut für Technologie, Karlsruhe

<sup>20</sup>Korea Institute of Science and Technology Information, Daejeon

<sup>21</sup>Korea University, Seoul

<sup>22</sup>Kyoto University, Kyoto

<sup>23</sup>Kyungpook National University, Taegu

<sup>24</sup>École Polytechnique Fédérale de Lausanne (EPFL), Lausanne

<sup>25</sup>Faculty of Mathematics and Physics, University of Ljubljana, Ljubljana

<sup>26</sup>Luther College, Decorah, Iowa 52101

<sup>27</sup>University of Maribor, Maribor

<sup>28</sup>Max-Planck-Institut für Physik, München

<sup>29</sup>University of Melbourne, School of Physics, Victoria 3010

<sup>30</sup>Graduate School of Science, Nagoya University, Nagoya

<sup>31</sup>Kobayashi-Maskawa Institute, Nagoya University, Nagoya

<sup>32</sup>Nara Women's University, Nara

<sup>33</sup>National Central University, Chung-li

<sup>34</sup>National United University, Miao Li

- <sup>35</sup>Department of Physics, National Taiwan University, Taipei  
<sup>36</sup>H. Niewodniczanski Institute of Nuclear Physics, Krakow  
<sup>37</sup>Nippon Dental University, Niigata  
<sup>38</sup>Niigata University, Niigata  
<sup>39</sup>Osaka City University, Osaka  
<sup>40</sup>Osaka University, Osaka  
<sup>41</sup>Pacific Northwest National Laboratory, Richland, Washington 99352  
<sup>42</sup>Panjab University, Chandigarh  
<sup>43</sup>Research Center for Nuclear Physics, Osaka  
<sup>44</sup>University of Science and Technology of China, Hefei  
<sup>45</sup>Seoul National University, Seoul  
<sup>46</sup>Sungkyunkwan University, Suwon  
<sup>47</sup>School of Physics, University of Sydney, NSW 2006  
<sup>48</sup>Tata Institute of Fundamental Research, Mumbai  
<sup>49</sup>Excellence Cluster Universe, Technische Universität München, Garching  
<sup>50</sup>Tohoku Gakuin University, Tagajo  
<sup>51</sup>Tohoku University, Sendai  
<sup>52</sup>Department of Physics, University of Tokyo, Tokyo  
<sup>53</sup>Tokyo Institute of Technology, Tokyo  
<sup>54</sup>Tokyo Metropolitan University, Tokyo  
<sup>55</sup>Tokyo University of Agriculture and Technology, Tokyo  
<sup>56</sup>CNP, Virginia Polytechnic Institute and State University, Blacksburg, Virginia 24061  
<sup>57</sup>Yonsei University, Seoul  
<sup>58</sup>Research Center for Nuclear Physics, Osaka University, Osaka

(Dated: September 16, 2018)

We report the observation of two narrow structures in the mass spectra of the  $\pi^\pm \Upsilon(nS)$  ( $n = 1, 2, 3$ ) and  $\pi^\pm h_b(mP)$  ( $m = 1, 2$ ) pairs that are produced in association with a single charged pion in  $\Upsilon(5S)$  decays. The measured masses and widths of the two structures averaged over the five final states are  $M_1 = (10607.2 \pm 2.0) \text{ MeV}/c^2$ ,  $\Gamma_1 = (18.4 \pm 2.4) \text{ MeV}$  and  $M_2 = (10652.2 \pm 1.5) \text{ MeV}/c^2$ ,  $\Gamma_2 = (11.5 \pm 2.2) \text{ MeV}$ . The results are obtained with a  $121.4 \text{ fb}^{-1}$  data sample collected with the Belle detector in the vicinity of the  $\Upsilon(5S)$  resonance at the KEKB asymmetric-energy  $e^+e^-$  collider.

PACS numbers: 14.40.Pq, 13.25.Gv, 12.39.Pn

Recent studies of heavy quarkonium have produced a number of surprises and puzzles [1], including some associated with  $\Upsilon(5S)$  decays to non- $B\bar{B}$  final states. The Belle Collaboration reported the observation of anomalously high rates for  $\Upsilon(5S) \rightarrow \Upsilon(nS)\pi^+\pi^-$  ( $n = 1, 2, 3$ ) [2] and  $\Upsilon(5S) \rightarrow h_b(mP)\pi^+\pi^-$  ( $m = 1, 2$ ) [3] transitions. If the  $\Upsilon(nS)$  signals are attributed entirely to  $\Upsilon(5S)$  decays, the measured partial decay widths  $\Gamma[\Upsilon(5S) \rightarrow \Upsilon(nS)\pi^+\pi^-] \sim 0.5 \text{ MeV}$  are about two orders of magnitude larger than typical widths for dipion transitions among the four lower  $\Upsilon(nS)$  states. Furthermore, the processes  $\Upsilon(5S) \rightarrow h_b(mP)\pi^+\pi^-$ , which require a heavy-quark spin flip, are found to have rates that are comparable to those for the heavy-quark spin conserving transitions  $\Upsilon(5S) \rightarrow \Upsilon(nS)\pi^+\pi^-$  [3]. These observations differ from *a priori* theoretical expectations and strongly suggest that exotic mechanisms are contributing to  $\Upsilon(5S)$  decays. We report results of resonant substructure studies of  $\Upsilon(5S) \rightarrow \Upsilon(nS)\pi^+\pi^-$  ( $n = 1, 2, 3$ ) and  $\Upsilon(5S) \rightarrow h_b(mP)\pi^+\pi^-$  ( $m = 1, 2$ ) decays [4]. We use a  $121.4 \text{ fb}^{-1}$  data sample collected on or near the peak of the  $\Upsilon(5S)$  resonance ( $\sqrt{s} \sim 10.865 \text{ GeV}$ ) with the Belle detector at the KEKB asymmetric energy  $e^+e^-$  collider [5].

The Belle detector is a large-solid-angle magnetic spec-

trometer that consists of a silicon vertex detector, a central drift chamber, an array of aerogel threshold Cherenkov counters, a barrel-like arrangement of time-of-flight scintillation counters, and an electromagnetic calorimeter comprised of CsI(Tl) crystals located inside a superconducting solenoid that provides a  $1.5 \text{ T}$  magnetic field. An iron flux-return located outside the coil is instrumented to detect  $K_L^0$  mesons and to identify muons. The detector is described in detail elsewhere [6].

To reconstruct  $\Upsilon(5S) \rightarrow \Upsilon(nS)\pi^+\pi^-$ ,  $\Upsilon(nS) \rightarrow \mu^+\mu^-$  candidates we select events with four charged tracks with zero net charge that are consistent with coming from the interaction point. Charged pion and muon candidates are required to be positively identified. Exclusively reconstructed events are selected by the requirement  $|M_{\text{miss}}(\pi^+\pi^-) - M(\mu^+\mu^-)| < 0.2 \text{ GeV}/c^2$ , where  $M_{\text{miss}}(\pi^+\pi^-)$  is the missing mass recoiling against the  $\pi^+\pi^-$  system calculated as  $M_{\text{miss}}(\pi^+\pi^-) = \sqrt{(E_{\text{c.m.}} - E_{\pi^+\pi^-}^*)^2 - p_{\pi^+\pi^-}^{*2}}$ ,  $E_{\text{c.m.}}$  is the center-of-mass (c.m.) energy and  $E_{\pi^+\pi^-}^*$  and  $p_{\pi^+\pi^-}^*$  are the energy and momentum of the  $\pi^+\pi^-$  system measured in the c.m. frame. Candidate  $\Upsilon(5S) \rightarrow \Upsilon(nS)\pi^+\pi^-$  events are selected by requiring  $|M_{\text{miss}}(\pi^+\pi^-) - m_{\Upsilon(nS)}| < 0.05 \text{ GeV}/c^2$ , where  $m_{\Upsilon(nS)}$  is the mass of an  $\Upsilon(nS)$

state [7]. Sideband regions are defined as  $0.05 \text{ GeV}/c^2 < |M_{\text{miss}}(\pi^+\pi^-) - m_{\Upsilon(nS)}| < 0.10 \text{ GeV}/c^2$ . To remove background due to photon conversions in the innermost parts of the Belle detector we require  $M^2(\pi^+\pi^-) > 0.20/0.14/0.10 \text{ GeV}/c^2$  for a final state with an  $\Upsilon(1S)$ ,  $\Upsilon(2S)$ ,  $\Upsilon(3S)$ , respectively.

Amplitude analyses of the three-body  $\Upsilon(5S) \rightarrow \Upsilon(nS)\pi^+\pi^-$  decays reported here are performed by means of unbinned maximum likelihood fits to two-dimensional  $M^2[\Upsilon(nS)\pi^+]$  vs.  $M^2[\Upsilon(nS)\pi^-]$  Dalitz distributions. The fractions of signal events in the signal region are determined from fits to the corresponding  $M_{\text{miss}}(\pi^+\pi^-)$  spectrum and are found to be  $0.937 \pm 0.015(\text{stat.})$ ,  $0.940 \pm 0.007(\text{stat.})$ ,  $0.918 \pm 0.010(\text{stat.})$  for final states with  $\Upsilon(1S)$ ,  $\Upsilon(2S)$ ,  $\Upsilon(3S)$ , respectively. The variation of reconstruction efficiency across the Dalitz plot is determined from a GEANT-based MC simulation [8]. The distribution of background events is determined using events from the  $\Upsilon(nS)$  sidebands and found to be uniform (after efficiency correction) across the Dalitz plot.

Dalitz distributions of events in the  $\Upsilon(2S)$  sidebands and signal regions are shown in Figs. 1(a) and 1(b), respectively, where  $M(\Upsilon(nS)\pi)_{\text{max}}$  is the maximum invariant mass of the two  $\Upsilon(nS)\pi$  combinations. This is used to combine  $\Upsilon(nS)\pi^+$  and  $\Upsilon(nS)\pi^-$  events for visualization only. Two horizontal bands are evident in the  $\Upsilon(2S)\pi$  system near  $112.6 \text{ GeV}^2/c^4$  and  $113.3 \text{ GeV}^2/c^4$ , where the distortion from straight lines is due to interference with other intermediate states, as demonstrated below. One-dimensional invariant mass projections for events in the  $\Upsilon(nS)$  signal regions are shown in Fig. 2, where two peaks are observed in the  $\Upsilon(nS)\pi$  system near  $10.61 \text{ GeV}/c^2$  and  $10.65 \text{ GeV}/c^2$ . In the following we refer to these structures as  $Z_b(10610)$  and  $Z_b(10650)$ , respectively.

We parameterize the  $\Upsilon(5S) \rightarrow \Upsilon(nS)\pi^+\pi^-$  three-body decay amplitude by:

$$M = A_{Z_1} + A_{Z_2} + A_{f_0} + A_{f_2} + A_{\text{nr}}, \quad (1)$$

where  $A_{Z_1}$  and  $A_{Z_2}$  are amplitudes to account for contributions from the  $Z_b(10610)$  and  $Z_b(10650)$ , respectively. Here we assume that the dominant contributions come from amplitudes that preserve the orientation of the spin of the heavy quarkonium state and, thus, both pions in the cascade decay  $\Upsilon(5S) \rightarrow Z_b\pi \rightarrow \Upsilon(nS)\pi^+\pi^-$  are emitted in an  $S$ -wave with respect to the heavy quarkonium system. As demonstrated in Ref. [9], angular analyses support this assumption. Consequently, we parameterize the observed  $Z_b(10610)$  and  $Z_b(10650)$  peaks with an  $S$ -wave Breit-Wigner function  $BW(s, M, \Gamma) = \frac{\sqrt{M\Gamma}}{M^2 - s - iM\Gamma}$ , where we do not consider possible  $s$ -dependence of the resonance width. To account for the possibility of  $\Upsilon(5S)$  decay to both  $Z_b^+\pi^-$  and  $Z_b^-\pi^+$ , the amplitudes  $A_{Z_1}$  and  $A_{Z_2}$  are symmetrized

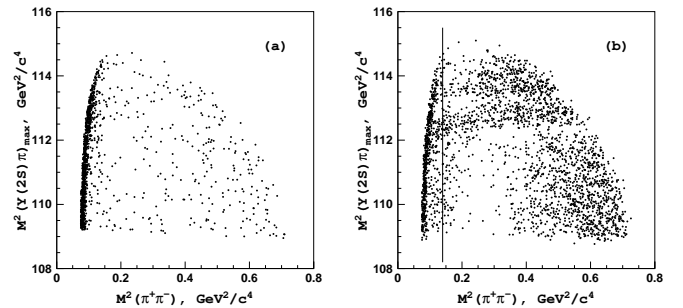


FIG. 1: Dalitz plots for  $\Upsilon(2S)\pi^+\pi^-$  events in the (a)  $\Upsilon(2S)$  sidebands; (b)  $\Upsilon(2S)$  signal region. Events to the left of the vertical line are excluded.

with respect to  $\pi^+$  and  $\pi^-$  transposition. Using isospin symmetry, the resulting amplitude is written as

$$A_{Z_k} = a_{Z_k} e^{i\delta_{Z_k}} (BW(s_1, M_k, \Gamma_k) + BW(s_2, M_k, \Gamma_k)), \quad (2)$$

where  $s_1 = M^2[\Upsilon(nS)\pi^+]$ ,  $s_2 = M^2[\Upsilon(nS)\pi^-]$ . The relative amplitudes  $a_{Z_k}$ , phases  $\delta_{Z_k}$ , masses  $M_k$  and widths  $\Gamma_k$  ( $k = 1, 2$ ) are free parameters. We also include the  $A_{f_0}$  and  $A_{f_2}$  amplitudes to account for possible contributions in the  $\pi^+\pi^-$  channel from the  $f_0(980)$  scalar and  $f_2(1270)$  tensor states, respectively. The inclusion of these two states is needed to describe the shape of the  $M(\pi^+\pi^-)$  spectrum around and above  $M(\pi^+\pi^-) = 1.0 \text{ GeV}/c^2$  for the  $\Upsilon(1S)\pi^+\pi^-$  final state (see Fig. 2). We use a Breit-Wigner function to parameterize the  $f_2(1270)$  and a coupled-channel Breit-Wigner function [10] for the  $f_0(980)$ . The mass and width of the  $f_2(1270)$  state are fixed at their world average values [7]; the mass and the coupling constants of the  $f_0(980)$  state are fixed at values determined from the analysis of  $B^+ \rightarrow K^+\pi^+\pi^-$ :  $M[f_0(980)] = 950 \text{ MeV}/c^2$ ,  $g_{K\pi} = 0.23$ ,  $g_{KK} = 0.73$  [11].

Following suggestions in Ref. [12], the non-resonant amplitude  $A_{\text{nr}}$  is parameterized as  $A_{\text{nr}} = a_1^{\text{nr}} e^{i\delta_1^{\text{nr}}} + a_2^{\text{nr}} e^{i\delta_2^{\text{nr}}} s_3$ , where  $s_3 = M^2(\pi^+\pi^-)$  ( $s_3$  is not an independent variable and can be expressed via  $s_1$  and  $s_2$  but we use it here for clarity),  $a_1^{\text{nr}}$ ,  $a_2^{\text{nr}}$ ,  $\delta_1^{\text{nr}}$  and  $\delta_2^{\text{nr}}$  are free parameters of the fit.

The logarithmic likelihood function  $\mathcal{L}$  is then constructed as

$$\mathcal{L} = -2 \sum \log(f_{\text{sig}} S(s_1, s_2) + (1 - f_{\text{sig}}) B(s_1, s_2)), \quad (3)$$

where  $S(s_1, s_2)$  is the density of signal events  $|M(s_1, s_2)|^2$  convolved with the detector resolution function,  $B(s_1, s_2)$  describes the combinatorial background that is considered to be constant and  $f_{\text{sig}}$  is the fraction of signal events in the data sample. Both  $S(s_1, s_2)$  and  $B(s_1, s_2)$  are efficiency corrected.

In the fit to the  $\Upsilon(1S)\pi^+\pi^-$  and  $\Upsilon(2S)\pi^+\pi^-$  samples, the amplitudes and phases of all of the components are allowed to float. However, in the  $\Upsilon(3S)\pi^+\pi^-$  samples the

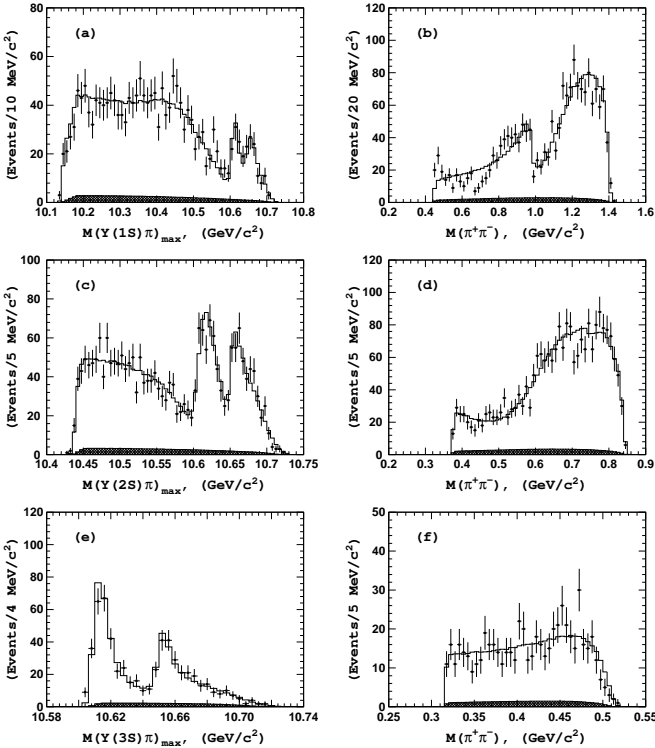


FIG. 2: Comparison of fit results (open histogram) with experimental data (points with error bars) for events in the  $\Upsilon(1S)$  (a,b),  $\Upsilon(2S)$  (c,d), and  $\Upsilon(3S)$  (e,f) signal regions. The hatched histogram shows the background component.

available phase space is significantly smaller and contributions from the  $f_0(980)$  and  $f_2(1270)$  channels are not well constrained. Since the fit to the  $\Upsilon(3S)\pi^+\pi^-$  signal is insensitive to the presence of these two components, we fix their amplitudes at zero. Due to the very limited phase space available in the  $\Upsilon(5S) \rightarrow \Upsilon(3S)\pi^+\pi^-$  decay, there is a significant overlap between the two processes  $\Upsilon(5S) \rightarrow Z_b^+\pi^-$  and  $\Upsilon(5S) \rightarrow Z_b^-\pi^+$ .

Results of the fits to  $\Upsilon(5S) \rightarrow \Upsilon(nS)\pi^+\pi^-$  signal events are shown in Fig. 2, where one-dimensional projections of the data and fits are compared. Numerical results are summarized in Table I, where the relative normalization is defined as  $a_{Z_2}/a_{Z_1}$  and the relative phase as  $\delta_{Z_2} - \delta_{Z_1}$ . The combined statistical significance of the two peaks exceeds  $10\sigma$  for all tested models and for all  $\Upsilon(nS)\pi^+\pi^-$  channels.

The main source of systematic uncertainties in the analysis of  $\Upsilon(5S) \rightarrow \Upsilon(nS)\pi^+\pi^-$  channels is due to uncertainties in the parameterization of the decay amplitude. We fit the data with modifications of the nominal model (described in Eq. 1). In particular, we vary the  $M(\pi^+\pi^-)$  dependence of the non-resonant amplitude  $A_{\text{nr}}$ , include a  $D$ -wave component into  $A_{\text{nr}}$ , include the  $f_0(600)$  state, etc. The variations in the extracted  $Z_b$  parameters determined from fits with modified models are taken as estimates of the model uncertainties. Other

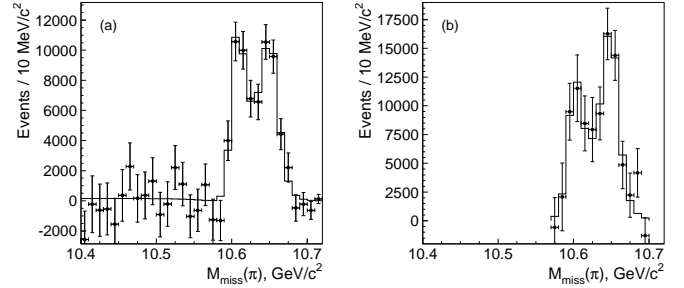


FIG. 3: The (a)  $h_b(1P)$  and (b)  $h_b(2P)$  yields as a function of  $M_{\text{miss}}(\pi)$  (points with error bars) and results of the fit (histogram).

major sources of systematic error include variation of the reconstruction efficiency over the Dalitz plot and uncertainty in the c.m. energy. Systematic effects associated with uncertainties in the description of the combinatorial background are found to be negligible. The overall systematic errors are quoted in Table I.

To study the resonant substructure of the  $\Upsilon(5S) \rightarrow h_b(mP)\pi^+\pi^-$  ( $m = 1, 2$ ) decays we measure their yield as a function of the  $h_b(1P)\pi^\pm$  invariant mass. The decays are reconstructed inclusively using the missing mass of the  $\pi^+\pi^-$  pair,  $M_{\text{miss}}(\pi^+\pi^-)$ . We fit the  $M_{\text{miss}}(\pi^+\pi^-)$  spectra in bins of  $h_b(1P)\pi^\pm$  invariant mass, defined as the missing mass of the opposite sign pion,  $M_{\text{miss}}(\pi^\mp)$ . We combine the  $M_{\text{miss}}(\pi^+\pi^-)$  spectra for the corresponding  $M_{\text{miss}}(\pi^+)$  and  $M_{\text{miss}}(\pi^-)$  bins and we use half of the available  $M_{\text{miss}}(\pi)$  range to avoid double counting.

Selection requirements and the  $M_{\text{miss}}(\pi^+\pi^-)$  fit procedure are described in detail in Ref. [3]. We consider all well reconstructed and positively identified  $\pi^+\pi^-$  pairs in the event. Continuum  $e^+e^- \rightarrow q\bar{q}$  ( $q = u, d, s$ ) background is suppressed by a requirement on the ratio of the second to zeroth Fox-Wolfram moments  $R_2 < 0.3$  [13]. The fit function is a sum of peaking components due to dipion transitions and combinatorial background. The positions of all peaking components are fixed to the values measured in Ref. [3]. In the case of the  $h_b(1P)$  the peaking components include signals from  $\Upsilon(5S) \rightarrow h_b(1P)$  and  $\Upsilon(5S) \rightarrow \Upsilon(2S)$  transitions, and a reflection from the  $\Upsilon(3S) \rightarrow \Upsilon(1S)$  transition, where the  $\Upsilon(3S)$  is produced inclusively or via initial state radiation. Since the  $\Upsilon(3S) \rightarrow \Upsilon(1S)$  reflection is not well constrained by the fits, we determine its normalization relative to the  $\Upsilon(5S) \rightarrow \Upsilon(2S)$  signal from the exclusive  $\mu^+\mu^-\pi^+\pi^-$  data for every  $M_{\text{miss}}(\pi)$  bin. In case of the  $h_b(2P)$  we use a smaller  $M_{\text{miss}}(\pi^+\pi^-)$  range than in Ref. [3],  $M_{\text{miss}}(\pi^+\pi^-) < 10.34 \text{ GeV}/c^2$ , to exclude the region of the  $K_S^0 \rightarrow \pi^+\pi^-$  reflection. The peaking components include the  $\Upsilon(5S) \rightarrow h_b(2P)$  signal and a  $\Upsilon(2S) \rightarrow \Upsilon(1S)$  reflection. To constrain the normalization of the  $\Upsilon(2S) \rightarrow \Upsilon(1S)$  reflection we use exclusive  $\mu^+\mu^-\pi^+\pi^-$  data normalized to the total yield of the

TABLE I: Comparison of results on  $Z_b(10610)$  and  $Z_b(10650)$  parameters obtained from  $\Upsilon(5S) \rightarrow \Upsilon(nS)\pi^+\pi^-$  ( $n = 1, 2, 3$ ) and  $\Upsilon(5S) \rightarrow h_b(mP)\pi^+\pi^-$  ( $m = 1, 2$ ) analyses.

Final state	$\Upsilon(1S)\pi^+\pi^-$	$\Upsilon(2S)\pi^+\pi^-$	$\Upsilon(3S)\pi^+\pi^-$	$h_b(1P)\pi^+\pi^-$	$h_b(2P)\pi^+\pi^-$
$M[Z_b(10610)]$ , MeV/ $c^2$	$10611 \pm 4 \pm 3$	$10609 \pm 2 \pm 3$	$10608 \pm 2 \pm 3$	$10605 \pm 2^{+3}_{-1}$	$10599^{+6+5}_{-3-4}$
$\Gamma[Z_b(10610)]$ , MeV	$22.3 \pm 7.7^{+3.0}_{-4.0}$	$24.2 \pm 3.1^{+2.0}_{-3.0}$	$17.6 \pm 3.0 \pm 3.0$	$11.4^{+4.5+2.1}_{-3.9-1.2}$	$13^{+10+9}_{-8-7}$
$M[Z_b(10650)]$ , MeV/ $c^2$	$10657 \pm 6 \pm 3$	$10651 \pm 2 \pm 3$	$10652 \pm 1 \pm 2$	$10654 \pm 3^{+1}_{-2}$	$10651^{+2+3}_{-3-2}$
$\Gamma[Z_b(10650)]$ , MeV	$16.3 \pm 9.8^{+6.0}_{-2.0}$	$13.3 \pm 3.3^{+4.0}_{-3.0}$	$8.4 \pm 2.0 \pm 2.0$	$20.9^{+5.4+2.1}_{-4.7-5.7}$	$19 \pm 7^{+11}_{-7}$
Rel. normalization	$0.57 \pm 0.21^{+0.19}_{-0.04}$	$0.86 \pm 0.11^{+0.04}_{-0.10}$	$0.96 \pm 0.14^{+0.08}_{-0.05}$	$1.39 \pm 0.37^{+0.05}_{-0.15}$	$1.6^{+0.6+0.4}_{-0.4-0.6}$
Rel. phase, degrees	$58 \pm 43^{+4}_{-9}$	$-13 \pm 13^{+17}_{-8}$	$-9 \pm 19^{+11}_{-26}$	$187^{+44+3}_{-57-12}$	$181^{+65+74}_{-105-109}$

reflection in the inclusive data. Systematic uncertainty in the latter number is included in the error propagation. The combinatorial background is parameterized by a Chebyshev polynomial. We use orders between 6 and 10 for the  $h_b(1P)$  [the order decreases monotonically with the  $M_{\text{miss}}(\pi)$ ] and orders between 6 and 8 for the  $h_b(2P)$ .

The results for the yield of  $\Upsilon(5S) \rightarrow h_b(mP)\pi^+\pi^-$  ( $m = 1, 2$ ) decays as a function of the  $M_{\text{miss}}(\pi)$  are shown in Fig. 3. The distribution for the  $h_b(1P)$  exhibits a clear two-peak structure without a significant non-resonant contribution. The distribution for the  $h_b(2P)$  is consistent with the above picture, though the available phase-space is smaller and uncertainties are larger. We associate the two peaks with the production of the  $Z_b(10610)$  and  $Z_b(10650)$ . To fit the  $M_{\text{miss}}(\pi)$  distributions we use the expression

$$|BW_1(s, M_1, \Gamma_1) + ac^{i\phi}BW_1(s, M_2, \Gamma_2) + be^{i\psi}|^2 \frac{qp}{\sqrt{s}}. \quad (4)$$

Here  $\sqrt{s} \equiv M_{\text{miss}}(\pi)$ ; the variables  $M_k$ ,  $\Gamma_k$  ( $k = 1, 2$ ),  $a$ ,  $\phi$ ,  $b$  and  $\psi$  are free parameters;  $\frac{qp}{\sqrt{s}}$  is a phase-space factor, where  $p$  ( $q$ ) is the momentum of the pion originating from the  $\Upsilon(5S)$  ( $Z_b$ ) decay measured in the rest frame of the corresponding mother particle. The  $P$ -wave Breit-Wigner amplitude is expressed as  $BW_1(s, M, \Gamma) = \frac{\sqrt{M\Gamma}F(q/q_0)}{M^2 - s - iM\Gamma}$ . Here  $F$  is the  $P$ -wave Blatt-Weisskopf form factor  $F = \sqrt{\frac{1+(q_0R)^2}{1+(qR)^2}}$  [14],  $q_0$  is a daughter momentum calculated with pole mass of its mother,  $R = 1.6 \text{ GeV}^{-1}$ . The function (Eq. 4) is convolved with the detector resolution function ( $\sigma = 5.2 \text{ MeV}/c^2$ ), integrated over the  $10 \text{ MeV}/c^2$  histogram bin and corrected for the reconstruction efficiency. The fit results are shown as solid histograms in Fig. 3 and are summarized in Table I. We find that the non-resonant contribution is consistent with zero [significance is  $0.3\sigma$  both for the  $h_b(1P)$  and  $h_b(2P)$ ] in accord with the expectation that it is suppressed due to heavy quark spin-flip. In case of the  $h_b(2P)$  we improve the stability of the fit by fixing the non-resonant amplitude to zero. The C.L. of the fit is  $81\%$  ( $61\%$ ) for the  $h_b(1P)$  [ $h_b(2P)$ ]. The default fit hypothesis is favored over the phase-space fit hypothesis at the  $18\sigma$  [ $6.7\sigma$ ] level for the  $h_b(1P)$  [ $h_b(2P)$ ].

To estimate the systematic uncertainty we vary the order of the Chebyshev polynomial in the fits to the  $M_{\text{miss}}(\pi^+\pi^-)$  spectra; to study the effect of finite  $M_{\text{miss}}(\pi)$  binning we shift the binning by half bin size; to study the model uncertainty in the fits to the  $M_{\text{miss}}(\pi)$  distributions we remove [add] the non-resonant contribution in the  $h_b(1P)$  [ $h_b(2P)$ ] case; we increase the width of the resolution function by 10% to account for possible difference between data and MC simulation. The maximum change of parameters for each source is used as an estimate of its associated systematic error. We estimate an additional  $1 \text{ MeV}/c^2$  uncertainty in mass measurements based on the difference between the observed  $\Upsilon(nS)$  peak positions and their world averages [3]. The total systematic uncertainty presented in Table I is the sum in quadrature of contributions from all sources. The significance of the  $Z_b(10610)$  and  $Z_b(10650)$  including systematic uncertainties is  $16.0\sigma$  [ $5.6\sigma$ ] for the  $h_b(1P)$  [ $h_b(2P)$ ].

In conclusion, we have observed two charged bottomonium-like resonances, the  $Z_b(10610)$  and  $Z_b(10650)$ , with signals in five different decay channels,  $\Upsilon(nS)\pi^\pm$  ( $n = 1, 2, 3$ ) and  $h_b(mP)\pi^\pm$  ( $m = 1, 2$ ). The parameters of the resonances are given in Table I. All channels yield consistent results. Weighted averages over all five channels give  $M = 10607.2 \pm 2.0 \text{ MeV}/c^2$ ,  $\Gamma = 18.4 \pm 2.4 \text{ MeV}$  for the  $Z_b(10610)$  and  $M = 10652.2 \pm 1.5 \text{ MeV}/c^2$ ,  $\Gamma = 11.5 \pm 2.2 \text{ MeV}$  for the  $Z_b(10650)$ , where statistical and systematic errors are added in quadrature. The  $Z_b(10610)$  production rate is similar to that of the  $Z_b(10650)$  for each of the five decay channels. Their relative phase is consistent with zero for the final states with the  $\Upsilon(nS)$  and consistent with  $180$  degrees for the final states with  $h_b(mP)$ . Production of the  $Z_b$ 's saturates the  $\Upsilon(5S) \rightarrow h_b(mP)\pi^+\pi^-$  transitions and accounts for the high inclusive  $h_b(mS)$  production rate reported in Ref. [3]. Analyses of charged pion angular distributions [9] favor the  $J^P = 1^+$  spin-parity assignment for both the  $Z_b(10610)$  and  $Z_b(10650)$ . Since the  $\Upsilon(5S)$  has negative  $G$ -parity, the  $Z_b$  states have positive  $G$ -parity due to the emission of the pion.

The minimal quark content of the  $Z_b(10610)$  and

$Z_b(10650)$  is a four quark combination. The measured masses of these new states are a few  $\text{MeV}/c^2$  above the thresholds for the open beauty channels  $B^*\overline{B}$  ( $10604.6 \text{ MeV}/c^2$ ) and  $B^*\overline{B}^*$  ( $10650.2 \text{ MeV}/c^2$ ). This suggests a “molecular” nature of these new states, which might explain most of their observed properties [15]. The preliminary announcement of these results triggered intensive discussion of other possible interpretations [16–19].

We are grateful to Alexander Milstein of BINP and Mikhail Voloshin of University of Minnesota for fruitful discussions. We thank the KEKB group for excellent operation of the accelerator, the KEK cryogenics group for efficient solenoid operations, and the KEK computer group and the NII for valuable computing and SINET4 network support. We acknowledge support from MEXT, JSPS and Nagoya’s TLPRC (Japan); ARC and DIISR (Australia); NSFC (China); MSMT (Czechia); DST (India); MEST, NRF, NSDC of KISTI, and WCU (Korea); MNiSW (Poland); MES and RFAAE (Russia); ARRS (Slovenia); SNSF (Switzerland); NSC and MOE (Taiwan); and DOE and NSF (USA).

- 
- [4] In the text, for conciseness, we refer to the initial state as the  $\Upsilon(5S)$ . However it is possible that the final states we discuss have a source that is distinct from the  $\Upsilon(5S)$ ; see K.-F. Chen *et al.* (Belle Collaboration), Phys. Rev. D **82**, 091196R (2010).
  - [5] S. Kurokawa and E. Kikutani, Nucl. Instrum. Methods Phys. Res. Sect. A **499**, 1 (2003), and other papers included in this Volume.
  - [6] A. Abashian *et al.* (Belle Collaboration), Nucl. Instrum. Methods Phys. Res., Sect. A **479**, 117 (2002).
  - [7] K. Nakamura *et al.* (Particle Data Group), J. Phys. G **37**, 075021 (2010).
  - [8] R. Brun *et al.*, GEANT 3.21, CERN DD/EE/84-1, 1984.
  - [9] I. Adachi *et al.* (Belle Collaboration), arXiv:1105.4583 [hep-ex].
  - [10] S.M. Flatté, Phys. Lett. B **63**, 224 (1976).
  - [11] A. Garmash *et al.* (Belle Collaboration), Phys. Rev. Lett. **96**, 251803 (2006).
  - [12] M.B. Voloshin, Prog. Part. Nucl. Phys. **61**, 455 (2008). M.B. Voloshin, Phys. Rev. D **74**, 054022 (2006) and references therein.
  - [13] G.C. Fox and S. Wolfram, Phys. Rev. Lett. **41**, 1581 (1978).
  - [14] J. Blatt and V. Weisskopf, Theoretical Nuclear Physics, p.361, New York: John Wiley & Sons (1952).
  - [15] A.E. Bondar, A. Garmash, A.I. Milstein, R. Mizuk, M.B. Voloshin, Phys. Rev. D **84**, 054010 (2011).
  - [16] D.V. Bugg, arXiv:1105.5492.
  - [17] I.V. Danilkin, V.D. Orlovsky, Yu.A. Simonov, arXiv:1106.1552.
  - [18] C.Y. Cui *et al.*, arXiv:1107.1343.
  - [19] T. Guo, L. Cao, M.-Z. Zhou, H. Chen, arXiv:1106.2284.

- 
- [1] N. Brambilla *et al.*, Eur. Phys. J. C **71**, 1534 (2011).
  - [2] K.-F. Chen *et al.* (Belle Collaboration), Phys. Rev. Lett. **100**, 112001 (2008).
  - [3] I. Adachi *et al.* (Belle Collaboration), arXiv:1103.3419 [hep-ex].